1   Seasonal blooms of neutrophilic *Betaproteobacterial* Fe(II) oxidizers and *Chlorobi* in

2   iron-rich coal mine drainage sediments

3

4   Nia Blackwell[1*], William Perkins[1], Barbara Palumbo-Roe[2], Jenny Bearcock[2],

5   Jonathan R. Lloyd[3], Arwyn Edwards[1,4]

6

7   [1] Department of Geography and Earth Sciences, Aberystwyth University,

8   Aberystwyth, Ceredigion, SY23 3DB, UK

9   [2] British Geological Survey, Environmental Science Centre, Nicker Hill, Keyworth,

10   Nottingham, NG12 5GG, UK

11   [3] Williamson Research Centre for Molecular Environmental Science, School of Earth,

12   Atmospheric and Environmental Sciences, University of Manchester, Manchester,

13   UK

14   [4] Institute of Biological, Environment Rural Science (and Interdisciplinary Centre for

15   Environmental Microbiology, and Centre for Glaciology), Aberystwyth University,

16   Aberystwyth, UK

17

18   *Present address: Nia Blackwell, Center for Applied Geosciences, 12

19   Hoelderlinstrasse, Tuebingen, Germany, 72070

20

24   **Abstract**

25

26   Waters draining from flooded and abandoned coal mines in the South Wales Coalfield

27   (SWC), are substantial sources of pollution to the environment characterized by

28   circumneutral pH and elevated dissolved iron concentrations (>1 mg L^{-1}). The

29   discharged Fe precipitates to form Fe(III) (oxyhydr)oxides which sustain microbial

30   communities. However, while several studies have investigated the geochemistry of

31   mine drainage in the SWC, less is known about the microbial ecology of the sites

32   presenting a gap in our understanding of biogeochemical cycling and pollutant

33   turnover. This study investigated the biogeochemistry of the Ynysarwed mine adit in

34   the SWC. Samples were collected from nine locations within sediment at the mine

35   entrance from the upper and lower layers three times over one year for geochemical

36   and bacterial 16S rRNA gene sequence analysis. During winter, members of the

37   *Betaproteobacteria* bloomed in relative abundance (>40%) including the

38   microaerophilic Fe(II)-oxidizing genus *Gallionella*. A concomitant decrease in

39   *Chlorobi*-associated bacteria occurred, although by summer the community

40   composition resembled that observed in the previous autumn. Here, we provide the

41   first insights into the microbial ecology and seasonal dynamics of bacterial

42   communities of Fe(III)-rich deposits in the SWC and demonstrate that neutrophilic

43   Fe(II)-oxidizing bacteria are important and dynamic members of these communities.

44

45

46

Introduction

Iron is an abundant redox-active element that accounts for around 5% of the earth's crust (Faure 1998). The two main redox states in the environment are Fe(II) (ferrous iron) and Fe(III) (ferric iron) which play a crucial role in many environmental biogeochemical cycles including nitrogen, sulfur, and carbon (Melton $et\ al.$ 2014). There are numerous biotic and abiotic reactions in the Fe biogeochemical cycle that involve the oxidation of Fe(II) to Fe(III) to form Fe(III) (oxyhydr)oxide precipitates and the reduction of Fe(III) to Fe(II) (Melton $et\ al.$ 2014). At circumneutral pH, Fe(II) is rapidly oxidized to Fe(III) by O_2 (Stumm and Morgan 1993) though this abiotic oxidation decreases substantially with decreasing O_2 concentrations, pH and temperature (Neubauer, Emerson and Megonigal 2002; Hedrich, Schlömann and Barrie Johnson 2011; Emerson $et\ al.$ 2015). In the presence of reduced sulfur species such as H_2S, Fe(III) (oxyhydr)oxides are abiotically reduced (Canfield 1989; Yao and Millero 1996). Microbially-mediated Fe(III) reduction involves reduction of Fe(III) by microorganisms that can use either H_2 or organic carbon as an electron donor (Lovley and Phillips 1988; Lovley 1997). At circumneutral pH, microorganisms capable of Fe(II) oxidation can be divided into three physiological groups: (i) anoxygenic nitrate-reducing, (Kappler, Schink and Newman 2005; Laufer $et\ al.$ 2016c), (ii) anoxygenic phototrophic (Widdel $et\ al.$ 1993), and (iii) microaerophilic (Emerson and Moyer 1997), the activities of which leads to the production of a variety of biogenic Fe(III) minerals (Bryce $et\ al.$ 2018).

The occurrence of Fe(III) (oxyhydr)oxide minerals is widespread in many environments, at both acidic and circumneutral pH, which allows for the development

3

72   of complex microbial communities with a range of metabolic activities that are

73   capable of cycling Fe (Peine *et al.* 2000; Duckworth *et al.* 2009; Wang *et al.* 2009;

74   Coby *et al.* 2011; Roden *et al.* 2012). More recent studies have focused on the

75   temporal changes in microbial communities in Fe(III)-rich environments (Fabisch *et*

76   *al.* 2013, 2016; Fleming *et al.* 2014). In environments where Fe cycling occurs, a

77   vertically stratified microbial community may develop due to the formation of redox

78   gradients (Duckworth *et al.* 2009). A theoretical framework for the distribution of Fe-

79   cycling microbes based on the prevailing environmental conditions, thermodynamic

80   and kinetic parameters, and the formation of geochemical niches has been proposed

81   (Schmidt, Behrens and Kappler 2010). However, the distribution of Fe-cycling

82   microbes can also be decoupled from geochemical gradients due to bioturbation,

83   metabolic flexibility, the occurrence of microniches and habitats, or interrelationships

84   with other microbial community members (Laufer *et al.*, 2016; Otte *et al.*, 2018).

85

86   The temporal dynamics of Fe cycling affects the occurrence, abundance, and

87   persistence of reactive Fe(III) oxides in sediments (Roden 2012). This in turn affects

88   the fate of other contaminants and metals, as Fe(III) (oxyhydr)oxide surfaces are

89   known for their strong sorption capacity (Gadd 2004; Borch *et al.* 2010) and can

90   affect the speciation and mobility of toxic contaminants (Vaughan and Lloyd 2011).

91   Metals and contaminants associated with Fe(III) (oxyhydr)oxides (either incorporated

92   into the structure or adsorbed to the surface) can be released during microbial

93   reduction (Smedley and Kinniburgh, 2002; Lloyd, 2003; Rhine *et al.*, 2005). Arsenic

94   is a problematic metalloid in many lakes, rivers, and aquifers and is detrimental to

95   human health (Brammer and Ravenscroft 2009; Smedley and Kinniburgh 2013;

96   Muehe and Kappler 2014). The role of Fe cycling in As mobilization has been a

4

97   major focus of several studies and the activities of several bacteria have been shown

98   to release As into the environment via Fe(III) mineral reductive mechanisms

99   (Cummings *et al.*, 1999; Islam *et al.*, 2004). Conversely, Fe(II)-oxidizing bacteria can

100 have a positive impact on the sequestration and removal of As from solution through

101 the production of biogenic Fe(III) minerals. Numerous field and laboratory studies

102 have shown the ability of Fe(III) (oxyhydr)oxides to act as sorbents for As (e.g. Dixit

103 and Hering, 2003; Hohmann *et al.*, 2010; Keim, 2011), especially in circumneutral

104 environments (Sowers *et al.* 2017). Therefore, identifying Fe-cycling microbial

105 communities present in contaminated environments, such as abandoned mines, is

106 imperative. Furthermore, understanding the temporal changes in microbial

107 communities associated with Fe(III)-rich environments is critical and has wider

108 implications on contaminant dynamics.

109

110 The South Wales Coalfield (SWC), UK, has a long history of mining activity, mainly

111 for the high-grade anthracitic coal. However, some of the worked coal seams contain

112 elevated concentrations of pyrite and arsenopyrite (2-4% pyritic S) (Evans, Watkins

113 and Banwart 2006), and consequently the discharge from many of the abandoned

114 mines is contaminated with Fe and, occasionally, As (Sapsford *et al.* 2015). The pH

115 of these mine waters is typically circumneutral due to the buffering capacity of the

116 underlying geology and, as such, Fe(III)-rich ochreous deposits are widespread within

117 the SWC. In recent years there have been several studies investigating the

118 geochemistry of these mines (Lewis, Leighfield and Cox 2000; Robins, Davies and

119 Dumpleton 2008; Farr *et al.* 2016). With the exception of a cultivation-based study

120 investigating moderate acidophiles in which isolates closely related to the thiosulfate-

121 oxidizing *Thiomas thermosulfata* were enriched (Hallberg and Johnson 2003), the

122   microbial communities of these ochreous deposits have not been investigated.

123   Furthermore, the impacts of these communities on the fate of contaminants and the

124   seasonal dynamics of microbial communities at these sites remain poorly understood.

125

126   Therefore, the aims of this study were to investigate the changes in the bacterial

127   community structure according to spatial, temporal, and environmental factors within

128   an Fe(III)-rich deposit at an abandoned coal mine, Ynysarwed, in the SWC. This site

129   is of particular interest due to the initial acidic and polluted discharge outburst (pH

130   3.2; 200-400 mg Fe L^{-1}) following a rebound in the water table in 1993 which resulted

131   in the pollution of the local hydrological system (Younger, 1997), and also the

132   occurrence of the Fe(II)/Fe(III) (oxyhydr)oxide green rust found in the ochreous

133   deposits (Bearcock *et al.* 2007). A high resolution sampling strategy was employed

134   for geochemical and bacterial 16S rRNA gene sequence analysis. Samples were

135   collected from nine locations within the ochreous deposit from both the upper and

136   lower layers of sediment. Our results show that bacterial communities within the

137   Fe(III)-rich deposit are dynamic and vary both spatially and temporally with several

138   operational taxonomic units (OTUs) closely related to known Fe-cycling bacteria;

139   their activity and potential influence on biogeochemical cycling and pollutant

140   sequestration is discussed.

141

142   **Methods**

143   *Field Site*

144   The SWC is an elongate, synformal structure of Carboniferous Coal Measures ~35

145   km north-south and ~80 km east-west covering an area of approximately 2690 km^2

146   (Bearcock *et al.* 2007; Farr *et al.* 2016) (Figure 1). The geology of the region consists

147   of faulted mudstones, sandstones, siltstones, and coals of the Lower, Middle, and

148   Upper Coal Measures deposited during the Westphalian Stage (Evans, Watkins and

149   Banwart 2006). This is underlain by the Namurian age Marros Group, previously

150   known as the Millstone Grit Series (Waters *et al.* 2009), and the Carboniferous

151   Limestone Beds. Many coal seams in this area were deposited under marine

152   conditions (Davies, Guion and Gutteridge 2012) and consequently have high pyrite

153   content of around 2-4% (Evans, Watkins and Banwart 2006).

154

155   The Ynysarwed mine adit (51°42'05.9"N, 3°43'33.1"W) (Figure 1) is situated in the

156   Lower Neath Valley and during operation mainly worked the notoriously pyritic

157   Rhondda No. 2 coal seam of the Upper Coal Measures. Although the mine water pH

158   is ~6 the total dissolved Fe concentrations are greater than the Water Framework

159   Directive guideline value (<1 mg L^{-1}) and elevated concentrations of total As in the

160   water (up to 30 µg L^{-1}) have been measured at the mine.

161

162   Samples were collected for geochemical and molecular biological analysis in autumn

163   (October 2011), winter (February 2012), and summer (July 2012). Nine locations (30-

164   40 cm between locations) within the Fe(III)-rich deposit (total depth ~40 cm) were

165   selected with samples collected from the upper (~5 cm) and lower (~30 cm) layers of

166   sediment from these locations (Figure 2).

167

168   *Geochemical Analysis*

169   Several physico-chemical parameters were measured in the field using unfiltered

170   water including pH, Eh, conductivity and temperature. pH and Eh were measured

171   using a calibrated HANNA HI 9025 microcomputer; for pH determination a

172   calibrated VWR probe was used (pH meter accuracy $\pm$ 0.01 pH units), and for Eh a Pt

173   wire combination sensor was used (Eh meter accuracy $\pm$ 1 mV). Temperature and

174   conductivity were measured using a calibrated HANNA HI 98312 Tester

175   (conductivity range 0-20 mS/cm $\pm$ 2% of measured value).

176

177   Mine water samples collected from the entrance of the adit were filtered immediately

178   in the field through a 0.22 μm Whatman® cellulose nitrate membrane filter and were

179   either acidified (pH <2) for cation analysis or left non-acidified for anion analysis.

180   Samples were transported in a cool box to the laboratory (<6 hours) where they were

181   then stored at 4 ˚C until analysis. Analysis of cations in solution was conducted on

182   duplicate samples either on a Perkin-Elmer AAnalyst 400 atomic absorption

183   spectrophotometer instrument or on an Agilent 7700x ICP-MS using tellurium or

184   ruthenium as the internal standard. Analysis of anions were conducted on duplicate

185   samples on a Dionex DX 100 ion chromatograph with an IonPac AS4A-SC analytical

186   column and were analysed within one week of sample collection.

187

188   Sediment samples for geochemical analysis were collected using a clean, sterilized

189   plastic scoop into sterile 50 mL Falcon™ tubes (Thermo Fisher Scientific Inc., UK).

190   Each tube was filled quickly leaving no headspace to avoid changes in the sediment

191   chemistry and were transported in a cool box back to the laboratory and stored at 4 ˚C

192   until analysis. Samples were subjected to centrifugation to remove excess water

193   before being air-dried, sieved <150 μm and sent to the British Geological Survey

194   (BGS), Keyworth, UK, for analysis of a suite of elements by ICP-MS (Agilent

195   7500cx quadrupole). A 0.25 g subsample of material was digested in perfluoroalkoxy

196   (PFA) beakers with a mixture of concentrated hydrofluoric (47-51%), perchloric (46-

197 49%) and nitric acid (67-69%) to a final volume of 25 mL and diluted 40-fold prior to

198 analysis. The final concentration of the nitric acid following dilution was 5%, with

199 trace amounts of hydrofluoric and perchloric acids. An internal standard solution

200 containing scandium, germanium, rhodium, indium, technetium and iridium was

201 added to the samples and instrument calibration standards. The standard reference

202 material BGS-102 (BGS, Ironstone soil, UK) was used as the certified reference

203 material (Wragg, 2009).

204

205 The Fe(II) weight % in the sediment was measured using a modification of Wilson's

206 (1955) classical titration method as described in Bearcock $et\ al.$ (2007). Porewater

207 was extracted from the sediment by centrifugation (5,000 x g for 10 minutes) and

208 subsequently filtered (<0.2 μm; Whatman® cellulose nitrate membrane). The

209 dissolved Fe(II) content of the pore water was determined using the Ferrozine assay

210 according to Stookey (1970) and measured on a Perkin-Elmer UV-Vis

211 spectrophotometer at 562 nm. The pH and weight % of organic matter (OM) in the

212 sediment was determined by analysis at the BGS. Briefly, soil pH was determined by

213 mixing a 5 g subsample of sieved sediment with a freshly prepared 0.1 M $CaCl_2$

214 solution at a ratio of 1:2.5 (w/v). The slurry was stirred for 5 minutes and allowed to

215 settle for at least 15 minutes before the pH measurement was determined using a

216 calibrated pH meter. To determine the weight percentage of OM the method of loss

217 on ignition (LOI) was used. A 1 g subsample of sediment was weighed into a crucible

218 (that had previously been weighed) and oven dried at 105 °C for at least 4 hours.

219 After cooling in a desiccator, the crucible and sediment were weighed again before

220 being heated in a furnace at 450 °C for at least 4 hours. Once cooled, the crucible and

221   sediment were weighed again and the weight percentage of OM in the sediment

222   calculated.

223

224   *Mineralogical Analysis*

225   To determine the mineralogy of the ochreous sediment - specifically the Fe minerals

226   present - samples were analysed by X-ray diffraction (XRD) and environmental

227   scanning electron microscopy (ESEM). For ESEM samples do not have to be dried

228   and this method was selected to avoid any artificial changes that may occur within the

229   sample during the drying process. For XRD analysis, an air dried sample of the

230   sediment was gently disaggregated in an agate pestle and mortar and the powder was

231   loaded onto a poly(methyl methacrylate) sample holder. The sample was analysed

232   using a Bruker D8 Advance X-ray diffractometer with a Vantec Super Speed detector

233   and Cu Kα radiation (1.542Å). The system was set up with a step size of 0.007° 2θ

234   and the scan speed was 0.01 seconds per step. The results were analysed using the

235   Diffrac.EVA software (Bruker, Billerica, Massachusetts). Analysis of samples by

236   ESEM took place at the School of Earth and Environmental Sciences at the University

237   of Manchester, UK, using a Philips XL30 ESEM-FG instrument. Slurried samples

238   were mounted onto 12.7 mm (0.5 inch) aluminium stubs using double-sided adhesive

239   tape in an anoxic chamber (100% N_2) to avoid oxidation of the sample during

240   preparation. Samples were transported within an airtight, oxygen-free container

241   before being loaded into the instrument. Samples were analysed at pressures between

242   0.5 and 0.6 torr using an accelerating voltage of 20 kV.

243

244   *Microbiological Sampling*

10

245   Sediment samples for microbiological analysis were collected using a clean plastic

246   scoop. A sterile spatula was used to transfer an aliquot of the scooped sample into a

247   sterile 50 mL Falcon™ tube. The tubes were filled to avoid headspace and thus the

248   introduction of oxygen into the sample and stored in the dark at ~4 °C whilst

249   transported back to the laboratory and stored at -20 °C prior to DNA extraction.

250

251   *High Throughput Semi-conductor Amplicon Sequencing of partial 16S rRNA genes*

252   Community DNA was extracted using the PowerSoil DNA extraction kit (MO BIO

253   Laboratories INC, CA, USA) according to the manufacturer's instructions. Samples –

254   a total of 54 – were then amplified for semi-conductor sequencing using the 27F (5′-

255   AGAGTTTGATCMTGGCTCAG) (Lane 1991) and 357R (5′-

256   CTGCTGCCTYCCGTA) (Klindworth *et al.* 2013) bacterial primer combination

257   spanning the V1-V2 hypervariable region of the 16S rRNA gene. Sequencing

258   adapters and barcodes (Whiteley *et al.* 2012) were incorporated into the forward and

259   reverse primers. Amplicons were cleaned using the AmPure® XP PCR purification

260   kit (Beckman-Coulter, Massachusetts). DNA concentrations were measured using a

261   NanoDrop ND-1000 UV-visible spectrophotometer and samples were normalized

262   before pooling. The quality of the cleaned amplicons was tested by running the

263   samples through an E-Gel® SizeSelect™ 2% Agarose gel on the E-Gel® System

264   (Life Technologies Ltd, Paisley, UK) and DNA fragments smaller than 400 bp were

265   removed. The DNA was quantified on an Agilent 2100 Bioanalyzer with a High

266   Sensitivity DNA chip (Agilent Technologies UK Ltd, Stockport, UK) and diluted to

267   26 pmol L^{-1} in preparation for emulsion PCR. Emulsion PCR was conducted using the

268   Ion PGM™ Template OT2 Reagents 400 kit 2.0 according to the manufacturer's

269   guidelines on an Ion One Touch™ 2 System and was set up as per the manufacturer's

270   guidelines (Life Technologies). Finally, the emulsion PCR amplified solution was

271   loaded onto an Ion 316™ Chip and run on the Ion Torrent PGM sequencer at the

272   Institute of Biological, Environmental and Rural Sciences, Aberystwyth University,

273   UK. The data were subjected to quality filtering (Ion Torrent default quality score

274   setting <15 over a window size of 30 nt) before the data were exported as FASTQ

275   files.

276

277   Sequences were analysed using QIIME v.1.7.0 (Caporaso *et al.*, 2010). Briefly, the

278   demultiplexed FASTQ files were labelled and filtered to remove any sequences

279   smaller than 300 bp. The samples were then clustered into operational taxonomic

280   units (OTUs) (default settings of 0.97 sequence similarity) using the UCLUST

281   algorithm (Edgar 2010). A representative OTU was identified using the Greengenes

282   database v.13_8 (DeSantis *et al.* 2006) using the Ribosomal Database Project (RDP)

283   classifier algorithm (Cole *et al.* 2009) at 97% sequence similarity. The sequences

284   were aligned against the Greengenes reference core imputed alignment (available

285   from Greengenes website) using the PyNAST alignment method (Caporaso *et al.*,

286   2010). Following this the data were checked for chimeric sequences using

287   ChimeraSlayer (Haas *et al.* 2011) available in QIIME before they were removed via

288   filtering. To visualise the data OTU tables were constructed and different filtering

289   techniques (e.g. removal of singletons and sequences that accounted for less than

290   0.1% of the total microbial community) were used. In total over 2 million reads were

291   generated for the 54 samples. A read count heatmap generated in QIIME was

292   exported to MS Excel to produce graphical plots. Raw data have been deposited at the

293   sequence read archive (SRA) under project number PRJNA521102.

294

295 *Statistical Analyses*

296 Environmental and microbiological data were exported into PRIMER software

297 (version 6.1.12; Primer-E, Ivybridge, UK) with the PERMANOVA+ (version 1.0.2)

298 add on for statistical analysis. Environmental data were normalized and a Euclidean

299 distance matrix constructed. For microbiological samples, data from the read count

300 heatmap produced in QIIME was exported to MS Excel and the relative abundance of

301 the OTUs as a percentage of the total bacterial community calculated. A Bray-Curtis

302 resemblance matrix was constructed using fourth root transformed relative abundance

303 data. PERMANOVA (Anderson 2001; Anderson and Willis 2003) was conducted

304 using default settings with 9999 permutations for single factor analysis and reduced

305 permutations for multi factor analysis while canonical analysis of principal

306 coordinates (CAP) in PERMANOVA+ was conducted using default settings. Alpha

307 diversity metrics including Chao1 (Chao 1984), Gini Index (Wittebolle *et al.* 2009),

308 Good's Coverage (Good 1953), Observed Species (Kuczynski *et al.* 2011), and the

309 Shannon Index (Shannon 1948), were calculated using the QIIME workflow scripts.

310

311 Distance based linear modeling was used to investigate the relationship between

312 changes in bacterial community composition and environmental variable predictors

313 using the PRIMER software. Environmental parameters included sediment digestion

314 data, OM content, pH and Fe(II) porewater data.

315

316 *PHREEQC Geochemical Modeling*

317 PHREEQC v2.18 (Parkhurst and Appelo 1999) geochemical modeling software and

318 the WATEQ4F database (Ball and Nordstrom 1991) were used to test the analytical

319 quality and completeness of the geochemical data set (electrical balance variation

320   <0.1%). The saturation index of various minerals and the speciation of contaminants

321   of interest were also determined.

322

323   **Results**

324

325   *Geochemical Analysis*

326   Generally, the pH of the water flowing above the sediment remained circumneutral

327   throughout the sampling period (pH ~6.2) (Table 1). For all sampling seasons the

328   concentration of total Fe in the mine water remained consistently elevated ($> 47 \pm 1.4$

329   mg L^{-1}) and was greatest in autumn while the concentration of total As was greater in

330   summer at 29.7 ± 0.4 µg L^{-1} (Table 1). PHREEQC analysis showed that up to 99 % of

331   the total As and >99 % of the total Fe were present in the their reduced forms.

332

333   Iron was the major component in the sediment (up to 64%) with the lowest values

334   seen in autumn and the highest in winter and summer (Table 1; Table S1). The same

335   was also true for the pH of the sediment (Table 1). Conversely, while the As in

336   sediment was elevated throughout (>1200 mg kg^{-1}) it was highest in autumn and

337   lowest in winter and summer (Table 1). The OM weight % of the sediment varied

338   seasonally with the greatest OM content observed during autumn (mean of 16%;

339   Table 1) before decreasing slightly in winter and again in summer (mean of 7%). The

340   greatest percentage of OM was observed during autumn at location 4 in the upper

341   sediments, along the left side of the deposit (Figure 2), and was present at double the

342   concentration of the surrounding samples at 34% (Table S1). Similar to the OM

343   results, Fe(II) concentrations in porewater were also typically higher in autumn and

344   winter (Table 1) and had decreased by the summer apart from a localized area in the

14

345   centre of the deposit (mean Fe(II) concentration 52.5 mg L^{-1} for locations 4, 5, 6 and 8

346   in the lower sediments). Generally, for all months samples at the front of the sampling

347   grid (i.e. locations 1-3) and in the upper sediments had lower Fe(II) porewater

348   concentrations (Figure 2; Table S1).

349

350   *Mineralogical Analysis*

351   Identification of the sediment by XRD showed the occurrence of the Fe(III)

352   (oxyhydr)oxide mineral goethite (α-FeOOH) at the mine site and this was true for all

353   sediment samples collected between autumn and summer (Figure S1). E-SEM

354   images show poorly crystalline Fe minerals and twisted *Gallionella*-like stalks (e.g.

355   Ionescu *et al.*, 2015; Fabisch *et al.*, 2016) as well as hollow structures reminiscent of

356   biogenic Fe(III) mineral morphotypes formed by other Fe(II)-oxidizing bacteria (e.g.

357   Fleming *et al.*, 2011, 2014; Chan *et al.*, 2016) (Figure 3).

358

359   *16S rRNA Gene Sequencing Profiles*

360   The results for the 16S rRNA gene sequencing of 54 samples from 9 locations in the

361   upper and lower deposit from the months of autumn, winter, and summer are shown

362   in Figure 4. Results are discussed in relative bacterial 16S rRNA sequence abundance

363   of OTUs as a proportion of the total number of reads per sample.

364

365   *Phylogenetic Diversity*

366   Samples were analysed for within-sample diversity (alpha) and between-sample

367   diversity (beta) at OTU level (Table 2). A calculation of Good's Coverage revealed

368   that all samples had coverage of 100. The mean Shannon-Weaver diversity index for

369   all samples was 3.3 and further analysis of samples by month did not deviate greatly

370   from this value (range 3.2 – 3.3).

371

372   *Taxonomic Composition*

373   At phylum level the *Proteobacteria* were the most dominant and accounted for 34%

374   of the total bacterial community (mean value for all 54 samples; Dataset S1). The

375   majority of the remaining population was comprised of bacteria affiliated with the

376   *Chlorobi* (33%) and *Bacteroidetes* (21%) phyla. Also present were lineages affiliated

377   to the phyla *Acidobacteria*, *Actinobacteria*, and *Nitrospirae*, though at a much lower

378   abundance (Dataset S1). Certain sequences represented lineages that were

379   unidentifiable at phylum level and accounted for 0.7 to 3.7% of the total community.

380   At class level the *Betaproteobacteria* were the most dominant and represented 25% of

381   total community on average. The *Chlorobi* were mainly represented by BSV6,

382   *Ignavibacteria* and OPB56. At genus level the *Betaproteobacteria* were mainly

383   comprised of several OTUs from the family *Comamonadaceae* including *Paucibacter*

384   and *Rhodoferax*. Also within the *Betaproteobacteria* were OTUs from the order

385   SBla14 and the Fe(II)-oxidizing genus *Gallionella*, whilst the order

386   *Desulfuromonadales* from the *Deltaproteobacteria* was represented entirely by the

387   genus *Geobacter* which contains known Fe(III)-reducing bacteria (Dataset S1).

388

389   *Variations in Taxonomic Composition According to Depth and Location*

390   Bacterial communities were sorted according to the sampling depth and location

391   regardless of the sampling month. At OTU level there was no significant difference

392   between locations for any month ($P >0.05$; Figure 5A), however, highly significant

393   differences between sample depths were observed ($P = 0.0002, 0.0001,$ and $0.0054,$

16

394   Pseudo-F = 15.54, 19.47, and 5.61 for autumn, winter, and summer, respectively). In

395   the upper sediment the dominant phyla were *Proteobacteria* (40%), *Chlorobi* (27%),

396   and *Bacteroidetes* (23%) (Figure S2). The same three phyla were dominant in the

397   lower sediments, however, the relative abundance of *Proteobacteria* decreased (27%),

398   while *Chlorobi* increased (40%) and *Bacteroidetes* remained consistent (20%).

399   Pairwise analysis for each of the three main phyla according to depth showed

400   significant differences (P <0.05; Table S2). OTUs within the order SB1a14 were

401   more abundant in the upper sediments (ranging 1-40%) compared to the lower

402   sediments (ranging 0.6-27%). The same was also true for OTUs from the genus

403   *Gallionella* (Dataset S1). OTUs classified as the Fe(III)-reducing bacteria-containing

404   genus *Geothrix* were evenly distributed (though at low abundance, ~1%).

405

406   *Seasonal Variations in Taxonomic Composition*

407   Generally, the community composition for autumn and summer were the most similar

408   based on the relative abundance of the most dominant phyla (Figure S3). Mean values

409   for each month (upper and lower sediments combined) showed that the abundance of

410   OTUs from the phylum *Proteobacteria* were similar in autumn and summer (28-

411   29%), which was also true for the *Chlorobi* (34-38%) (Figure S3). Samples collected

412   during winter, however, displayed a different composition and an increase in

413   *Proteobacteria* (to 42%) and a concomitant decrease in *Chlorobi* (to 27%) was

414   observed. Pairwise analysis of *Proteobacteria*- and *Chlorobi*-affiliated OTUs

415   according to months showed significant (P <0.05) differences between autumn versus

416   winter and winter versus summer, but not between autumn versus summer (Figure

417   5B; Table S2). A similar clustering of samples was observed when samples were

418   analysed non-metric dimensional scaling (nMDS) at OTU level (Figure S4). Further

419   investigation of the winter samples revealed that the increase in *Proteobacteria*

420   mainly occurred in the upper sediments (56%) compared to the lower sediment

421   (29%). One of the greatest variations in the *Proteobacteria* occurred within the

422   *Betaproteobacterial* order SB1a14 which increased up to 40% in certain samples

423   during winter (Figure 4), before decreasing again in summer. The same was also true

424   for *Gallionella*-affiliated OTUs. The decrease in *Chlorobi* in winter was particularly

425   apparent in the order VC38 (Figure 4) and the relationship between the relative

426   abundance of the *Chlorobi* order VC38 and *Betaproteobacteria* order SBla14

427   appeared to be closely linked (Figure 6).

428

429   Differences in community structure between neighbouring samples were also

430   apparent (Figure 4). However, at OTU level these differences were not statistically

431   significant during any month ($P > 0.3$). In relation to the grid sampling strategy a

432   general pattern was observed: between autumn and winter an increase in the relative

433   abundance of *Proteobacteria*-affiliated OTUs, especially order SBla14, occurred

434   within upper sediment samples collected along the front and left side of the adit

435   (locations 1-7; Fig. 2). This substantial increase in order SBla14 was also observed in

436   the lower sediments, though only in one sample at location 7. An increase in the

437   genus *Geobacter* was observed in upper sediment samples 1-7 during winter (Figure

438   4), for example the mean relative abundance ($n = 7$) during winter was 5% compared

439   to 3 and 1% in autumn and summer, respectively. This was also true for the genus

440   *Gallionella*, for example, at location 1 in the upper sediments the relative abundance

441   increased from 8% in autumn to 18% in winter before decreasing to 4% in summer.

442   Within the lesser represented taxa seasonal variations were also evident with a large

443   increase in a single OTU affiliated to the species *Variovorax paradoxans* (99% 16S

444 rRNA gene identity). At location 4 in the lower sediments during summer the relative

445 abundance of this OTU was 26% while for the remaining samples it was <1%.

446

447 **Discussion**

448

449 *Impacts of Historical Mining on Water Quality*

450 The occurrence of precipitated Fe(III) minerals at the Ynysarwed mine site is

451 indicative of the dissolution of pyrite that is present in the worked coal seams within

452 the mine (Evans, Watkins and Banwart 2006). During aerobic working conditions

453 highly soluble secondary minerals known as efflorescent salts (Nordstrom and Alpers

454 1999) such as melanterite ($FeSO_4 \cdot 7H_2O$), which has been found in many mines in the

455 SWC (Bevins 1994), likely formed on the surface of the seams (Robins, Davies and

456 Dumpleton 2008). Dissolution of these salts and further pyrite oxidation caused either

457 by microbially-mediated processes (Quatrini and Johnson 2018) or chemically by

458 strong oxidants such as Fe^{3+} (Johnson and Hallberg 2003) results in Fe- and sulfate-

459 rich mine waters as shown in the water chemistry data. Furthermore, the elevated total

460 As concentrations may indicate the presence and biodegradation of As-bearing ores

461 such as arsenopyrite, while the elevated Ca and Mg concentrations are due to the

462 occurrence of carbonate rocks, which is in agreement with the local geology. The

463 relationship between Fe minerals and contaminants is well documented e.g. Dzombak

464 and Morel (1990) and several studies have shown that Fe(III) (oxyhydr)oxides are

465 capable of sequestering As from solution through absorption or co-precipitation at

466 circumneutral pH (e.g. Adra *et al.*, 2013; Sowers *et al.*, 2017) which explains the

467 elevated concentrations of total As in the sediment.

468

469   *Bacterial Taxa Associated with Iron Cycling*

470   Lineages affiliated with those known to contain Fe-cycling microbes were found at

471   comparatively high relative abundances that changed seasonally. OTUs affiliated to

472   known Fe(III)-reducing bacteria genera include *Geothrix, Geobacter* and *Rhodoferax*.

473   An OTU demonstrating 99% 16S rRNA gene identity to *Rhodoferax ferrireducens*

474   (Finneran, Johnsen and Lovley 2003), a facultative anaerobe, was present in all

475   samples. *Geobacter* spp. are known Fe(III) reducers capable of coupling organic

476   carbon oxidation to Fe(III)-reduction (Lovley 1997; Islam *et al.* 2004). OTUs

477   affiliated to the *Geobacter* genus demonstrated 96% 16S rRNA gene identity across

478   the sequenced region to *Geobacter psychrophilus* (Nevin *et al.* 2005) and 98% 16S

479   rRNA gene similarity to clones of subsurface *Geobacter* communities stimulated by

480   acetate addition to a uranium contaminated aquifer (Elifantz *et al.* 2010).

481

482   Lineages affiliated to those containing known Fe(II)-oxidizing bacteria were also

483   present in relatively high abundances in the sediment. Microaerophilic Fe(II)

484   oxidizers, such as *Gallionella* spp., exist at the redox boundary of opposing gradients

485   of oxygen and Fe(II) (Emerson and Moyer 1997; Neubauer, Emerson and Megonigal

486   2002; Lueder *et al.* 2018). *Gallionella* spp. grow by using Fe(II) as the electron donor

487   and oxygen as the electron acceptor (Hallbeck and Pedersen 1991). They have also

488   been found to be surprisingly dominant under slightly acidic conditions (pH ~4)

489   (Fabisch *et al.* 2013). The sequences of the representative OTUs identified as

490   *Gallionella* spp. were verified by BLAST to identify the OTUs at species level. The

491   most abundant *Gallionella*-related OTUs shared the greatest gene sequence identity

492   with *Gallionella capsiferriformans* ES-2 (97-98% 16S rRNA gene sequence identity)

493   (Emerson *et al.* 2013) although OTUs present at lower abundances (<1%) were not as

494   similar (94-95%). The occurrence of Fe(II) oxidizers closely related to this species at

495   heavy metal contaminated sites has already been documented (Fabisch *et al.* 2016).

496   This may be explained by the presence of heavy metal efflux pumps found in the

497   genome as well as genes for arsenic resistance (Emerson *et al.* 2013). The general

498   greater relative abundance of microaerophilic *Gallionella*-related species in the upper

499   sediments (5 cm depth) also suggests a vertically stratified redox gradient within the

500   ochreous deposits, a phenomenon known to occur in Fe-cycling sediments

501   (Duckworth *et al*., 2009). The *Betaproteobacteria* order SBla14, which consisted of 3

502   OTUs, increased substantially during winter in the upper sediments particularly at

503   locations 1-7 at the front and left side of the adit. Further analysis of the dominant

504   OTUs within this order showed 95-97% 16S rRNA gene similarity to the Fe(II)-

505   oxidizing bacterium *Sideroxydans lithotrophicus* ES-1 (Emerson *et al.* 2013), and

506   99% 16S rRNA gene identity to clones obtained from "iron snow" particles present in

507   an acidic lignite mine lake (Reiche *et al.* 2011). While it is not possible to infer *in situ*

508   microbial function from partial 16S rRNA gene sequence data, it can be hypothesized

509   that the SBla14-affiliated OTUs are involved in Fe(II) oxidation. However, further

510   isolation and physiological studies are required to determine this.

511

512   *Ecological succession*

513   This research shows clear evidence for ecological succession between two of the most

514   abundant taxa at the field site. A concomitant change in the bacterial community was

515   observed in members of the *Chlorobi* order VC38 and members of the

516   *Betaproteobacteria* order SBla14 throughout the course of one year. *Chlorobi* VC38

517   OTUs dominated the communities in autumn, however, by winter *Betaproteobacteria*

518   SBla14 OTUs were the most dominant. By summer the community had returned to

519   almost the same community observed in autumn the previous year demonstrating a

520   cyclic transition between two principal community members. It can be hypothesized

521   that the increase in the putative Fe(II) oxidizer from the *S. lithotrophicus*-related

522   SBla14 during winter, especially in the upper sediments (up to 40%), is due to

523   conditions favourable for microaerophilic Fe(II) oxidation. This is also evident in the

524   increase in *Gallionella* for the same month. However, the role of OTUs related to the

525   *Chlorobi* VC38 remains unknown. Further analysis of the OTUs revealed little more

526   information (closest cultured relative <91% similarity), only that environmental

527   clones with no hypothesized function from an acid-impacted lake were closely related

528   (99% 16S rRNA gene similarity) (Percent *et al.* 2008). Members of the *Chlorobi* are

529   known for growth via anoxygenic photosynthesis, coupling the fixation of CO_2 into

530   biomass with the oxidation of reduced sulfur to replace the electrons lost from the

531   photosystem during carbon assimilation (Overmann 2006). However, certain

532   members of the *Chlorobi* phylum can grow by oxidizing Fe(II) (e.g. Crowe *et al.*,

533   2017), the so called photoferrotrophs (see Bryce *et al.*, 2018 for a comprehensive

534   review). If this is the case, the temporal transition from the putative microaerophilic

535   and anoxygenic photoferrotrophic metabolism could represent a phenomenon that has

536   yet to be described in circumneutral mine drainage environments. Currently, most

537   photoferrotrophic isolates have originated from either freshwater sediment and lakes

538   or marine sediments (Bryce *et al.* 2018). The occurrence of *Chlorobi* has been

539   reported in 16S rRNA gene sequencing surveys of acid mine drainage (Volant *et al.*

540   2014; Mesa *et al.* 2017) and soils impacted by circumneutral mine drainage (Pereira,

541   Vicentini and Ottoboni 2014) though at low abundance (<1%). It is possible that the

542   high relative abundance for *Chlorobi*-affiliated OTUs at Ynysarwed represents a

543   previously overlooked microbial metabolism in circumneutral mine drainage that can

544   greatly impact pollutant turnover.

545

546   While the ecological function of the dominant *Chlorobi*-affiliated OTU at the

547   Ynysarwed mine adit cannot be inferred from the partial 16S rRNA gene sequencing

548   data currently available, it highlights the need for cultivation-based approaches to

549   determine the metabolism of this particular bacterium, and may provide insight into

550   the type of growth conditions to be tested (i.e. anoxygenic photoferrotrophy). This

551   research demonstrates that there is likely a complex interplay between geochemical

552   and microbial factors that result in a seasonal ecological succession, and further

553   cultivation-dependent and metagenomics work could help to elucidate the role of the

554   *Chlorobi* VC38- and *Betaproteobacteria* SBla14-affiliated bacteria.

555

556   *Fluxes of Substrates Drives Biogeochemical Iron Cycling*

557   The OM content of the sediment varied seasonally and by location and is likely to

558   reflect the deposition of fallen leaves from nearby deciduous trees during winter

559   months. The particularly elevated concentration at location 4 in the upper sediments

560   compared to other samples indicates that this localized influx of OM is the case. The

561   occurrence of leaves in the sediment, particularly at the entrance of the adit, was

562   noted several times during fieldwork. The concentration of Fe(II) in pore waters

563   varied spatially and may be due to the influence of infiltrating oxygen from the

564   atmosphere into the sediments. This is shown by the comparatively lower

565   concentrations measured at the entrance of the adit at locations 1, 2 and 3.

566   Conversely, the localised area of comparatively elevated concentrations of Fe(II)

567   centred around location 5L may indicate the lack of oxygen infiltration to these parts.

568   Another possibility is that the influx of organic carbon stimulated the reduction of

569   bioavailable Fe(III) by Fe(III)-reducing microbes. Lineages affiliated to those known

570   to be capable of Fe(III) reduction were detected at relatively high abundances within

571   the sediment.

572

573   Although the greatest OM content was detected during autumn the change in the

574   bacterial community may not occur immediately. A possible reason for this includes a

575   delay period created by the time necessary for the catabolism of the complex organic

576   compounds by a certain taxon, or indeed several taxa, into more simple forms that can

577   be used by other microbes. This, therefore, also suggests the presence of a syntrophic

578   microbial community where microbes take advantage of the metabolic abilities of

579   their syntrophic partner (Schink 2002; Stams and Plugge 2009). At location 4 during

580   summer - the location with the greatest OM content measured in the study (in the

581   upper sediments in autumn at ~34%) - an increase in an OTU affiliated to the

582   bacterium *Variovorax paradoxus* (99% 16S rRNA gene sequence similarity) was

583   observed in the lower sediments. This species, a member of the family

584   *Comamonadaceae* within the *Proteobacteria* formerly known as *Alcaligenes*

585   *paradoxus* (Davis *et al.* 1969; Willems *et al.* 1991), has numerous metabolic

586   capabilities that are associated with important catabolic processes including the

587   degradation of toxic and complex chemical compounds. These include the

588   degradation of chitin, cellulose and humic acids (Satola, Wübbeler and Steinbüchel

589   2013). Several strains of *V. paradoxus* have been shown to participate in syntrophic

590   relationships with other plant and bacterial species (Satola, Wübbeler and Steinbüchel

591   2013). The importance of this bacterium in the degradation process of OM and also its

24

592   involvement in numerous syntrophic processes suggests that the increase in relative

593   abundance is due to the addition of OM to the sediment.

594

595   The substantial bacterial community changes observed at locations 1-7 in the upper

596   sediments during winter, specifically an increase in putative Fe(II) oxidizers from the

597   order SBla14, is likely due to the formation of additional Fe(II) by Fe(III) reducers.

598   Fe(III)-reducing bacteria have been shown to greatly impact and decrease the net

599   Fe(II) oxidation rate in natural sediments due to their rapid reduction rates (Laufer *et*

600   *al.*, 2016). This rapid reduction of Fe(III) would provide sufficient Fe(II) to support

601   microbial microaerophilic Fe(II) oxidation and during that time an increase in the

602   comparatively well characterized Fe(II)-oxidizing *Gallionella* was also observed.

603   Furthermore, the occurrence of OM plays an important role in the stabilization of

604   Fe(II) (Sundman *et al.* 2014; Bhattacharyya *et al.* 2018) by forming OM-Fe(II)

605   complexes which have been found in a range of environments (Kleja *et al.* 2012; von

606   der Heyden *et al.* 2014; Hopwood *et al.* 2015). Therefore, a decrease in abiotically

607   oxidized Fe(II) either by molecular oxygen or through heterogenous Fe(II) oxidation

608   (Park and Dempsey 2005; Melton *et al.* 2014) and an increase in OM-Fe(II)

609   complexes could provide a more stable substrate available for use by Fe(II)-oxidizing

610   bacteria. This, combined with a potential increase in the activity of Fe(III)-reducing

611   bacteria, could explain the bloom in abundance of putative Fe(II)-oxidizing bacteria at

612   the site.

613

614   *Implications for Contaminant Dynamics*

615   The formation, and also dissolution, of Fe(III) (oxyhydr)oxide minerals can have

616   substantial impacts on contaminant and nutrient dynamics (Islam *et al.* 2004; Borch *et*

617 *al.* 2010; Eickhoff *et al.* 2014). Therefore, the activity of Fe-cycling bacteria play a

618 major role in the sequestration and release of contaminants, such as As, in the

619 environment. Analysis of the sequence data showed a dramatic increase in OTUs

620 from the *Betaproteobacterial* order SBla14, a putative Fe(II)-oxidizing bacterium

621 related to *Sideroxydans lithotrophicus* ES-1, as well as *Gallionella*-related OTUs

622 during winter. This may have implications on the release of As from the mine site. As

623 previously discussed biogenic Fe(III) minerals are known strong sorbents and sinks

624 for As (Hohmann *et al.* 2010; Sowers *et al.* 2017) and therefore a bloom in Fe(II)-

625 oxidizing bacteria and subsequent Fe(III) biomineral production could increase the

626 sequestration of As from the mine water. This is not supported by the geochemical

627 water chemistry data as the concentration of As in solution increased slightly through

628 the sampling period. However, the processes, such as dissolution of As-bearing

629 minerals, and water retention times occurring within the flooded mine, upstream of

630 the mine adit, are unknown and might have masked the processes at the adit entrance.

631

632 *Conclusions and Outlook*

633 The geochemistry and relative bacterial 16S rRNA gene abundance of nine locations

634 within an Fe(III)-rich deposit at an abandoned coal mine in the SWC showed clear

635 differences between months, depths and locations. In autumn (October 2011) OTUs

636 closely related to *Chlorobi* VC38 which could potentially be an anoxygenic

637 photoferrotroph dominated, however, by winter (February 2012) the putative Fe(II)-

638 oxidizing *Betaproteobacteria* SBla14 related to *S. lithotrophicus* bloomed to

639 abundance. An increase in the well described Fe(II) oxidizer *Gallionella* was also

640 observed but to a lesser extent. By summer (July 2012) the community had returned

641 to almost the same community observed in the previous autumn demonstrating a

642 cyclic transition between two principal community members, possibly related to the

643 influx of OM to the sediment. This clear ecological succession highlights the

644 importance of spatial and temporal sampling strategies when investigating

645 environmental systems. The high relative abundance of the *Chlorobi*-affiliated OTUs

646 that currently have no known ecological function indicates the importance and

647 necessity of further investigations at this site, and also other sites in the SWC, to

648 include cultivation-dependent and metagenomics approaches to determine their

649 potential influence on contaminant and nutrient dynamics.

650

665   *Bibliography*

666   Adra A, Morin G, Ona-Nguema G *et al.* Arsenic Scavenging by Aluminum-

667   Substituted Ferrihydrites in a Circumneutral pH River Impacted by Acid Mine

668   Drainage. *Environ Sci Technol* 2013;**47**:12784–92.

669   Anderson MJ. A new method for non-parametric multivariate analysis of variance.

670   *Austral Ecol* 2001;**26**:32–46.

671   Anderson MJ, Willis TJ. Canonical Analysis of Principal Coordinates : A Useful

672   Method of Constrained Ordination for Ecology. *Ecology* 2003;**84**:511–25.

673   Ball JW, Nordstrom DK. *User's Manual for WATEQ4F , with Revised*

674   *Thermodynamic Data Base and Test Cases for Calculating Speciation of Major,*

675   *Trace, and Redox Elements in Natural Waters.*, 1991.

676   Bearcock JM, Perkins WT, Dinelli E *et al.* Fe(II)/Fe(III) 'green rust' developed within

677   ochreous coal mine drainage sediment in South Wales, UK. *Mineral Mag*

678   2007;**70**:731–41.

679   Bevins RE. *A Mineralogy of Wales*. National Museum Wales, 1994.

680   Bhattacharyya A, Schmidt MP, Stavitski E *et al.* Iron speciation in peats: Chemical

681   and spectroscopic evidence for the co-occurrence of ferric and ferrous iron in

682   organic complexes and mineral precipitates. *Org Geochem* 2018;**115**:124–37.

683   Borch T, Kretzschmar R, Kappler A *et al.* Biogeochemical Redox Processes and their

684   Impact on Contaminant Dynamics. *Environ Sci Technol* 2010;**44**:15–23.

685   Brammer H, Ravenscroft P. Arsenic in groundwater: A threat to sustainable

686   agriculture in South and South-east Asia. *Environ Int* 2009;**35**:647–54.

687   Bryce C, Blackwell N, Schmidt C *et al.* Microbial anaerobic Fe(II) oxidation -

688   Ecology, mechanisms and environmental implications. *Environ Microbiol*

689   2018;**20**:3462–83.

690   Canfield DE. Reactive iron in marine sediments. *Geochim Cosmochim Acta*

691   1989;**53**:619–32.

692   Caporaso JG, Bittinger K, Bushman FD *et al.* PyNAST: a flexible tool for aligning

693   sequences to a template alignment. *Bioinformatics* 2010a;**26**:266–7.

694   Caporaso JG, Kuczynski J, Stombaugh J *et al.* QIIME allows analysis of high-

695   throughput community sequencing data. *Nat Methods* 2010b;**7**:335–6.

696   Chan CS, McAllister SM, Leavitt AH *et al.* The architecture of iron microbial mats

697   reflects the adaptation of chemolithotrophic iron oxidation in freshwater and

698   marine environments. *Front Microbiol* 2016;**7**, DOI: 10.3389/fmicb.2016.00796.

699   Chao A. Nonparametric Estimation of the Number of Classes in a Population. *Scand J*

700   *Stat* 1984;**11**:265–70.

701   Coby AJ, Picardal F, Shelobolina E *et al.* Repeated anaerobic microbial redox cycling

702   of iron. *Appl Environ Microbiol* 2011;**77**:6036–42.

703   Cole JR, Wang Q, Cardenas E *et al.* The Ribosomal Database Project: improved

704   alignments and new tools for rRNA analysis. *Nucleic Acids Res* 2009;**37**:D141–

705   5.

706   Crowe SA, Hahn AS, Morgan-Lang C *et al.* Draft Genome Sequence of the Pelagic

707   Photoferrotroph Chlorobium phaeoferrooxidans. *Genome Announc*

708   2017;**5**:e01584-16.

709   Cummings DE, Caccavo F, Fendorf S *et al.* Arsenic mobilization by the dissimilatory

710   Fe(III)-reducing bacterium Shewanella alga BrY. *Environ Sci Technol*

711   1999;**33**:723–9.

712   Davies SJ, Guion PD, Gutteridge P. Carboniferous Sedimentation and Volcanism on

713   the Laurussian Margin. *Geological History of Britain and Ireland: Second*

714   *Edition*. 2012, 231–73.

715 Davis DH, Doudoroff M, Stanier RY *et al.* Proposal to reject the genus

716   Hydrogenomonas: Taxonomic implications. *Int J Syst Bacteriol* 1969;**19**:375–90.

717 DeSantis TZ, Hugenholtz P, Larsen N *et al.* Greengenes, a chimera-checked 16S

718   rRNA gene database and workbench compatible with ARB. *Appl Environ*

719   *Microbiol* 2006;**72**:5069–72.

720 Dixit S, Hering JG. Comparison of arsenic(V) and arsenic(III) sorption onto iron

721   oxide minerals: implications for arsenic mobility. *Environ Sci Technol*

722   2003;**37**:4182–9.

723 Duckworth OW, Holmström SJM, Peña J *et al.* Biogeochemistry of iron oxidation in

724   a circumneutral freshwater habitat. *Chem Geol* 2009;**260**:149–58.

725 Dzombak DA, Morel F. *Surface Complexation Modeling : Hydrous Ferric Oxide*.

726   Wiley, 1990.

727 Edgar RC. Search and clustering orders of magnitude faster than BLAST.

728   *Bioinformatics* 2010;**26**:2460–1.

729 Eickhoff M, Obst M, Schröder C *et al.* Nickel partitioning in biogenic and abiogenic

730   ferrihydrite: The influence of silica and implications for ancient environments.

731   *Geochim Cosmochim Acta* 2014;**140**, DOI: 10.1016/j.gca.2014.05.021.

732 Elifantz H, N'Guessan LA, Mouser PJ *et al.* Expression of acetate permease-like (apl)

733   genes in subsurface communities of Geobacter species under fluctuating acetate

734   concentrations. *FEMS Microbiol Ecol* 2010;**73**:no-no.

735 Emerson D, Field EK, Chertkov O *et al.* Comparative genomics of freshwater Fe-

736   oxidizing bacteria: implications for physiology, ecology, and systematics. *Front*

737   *Microbiol* 2013;**4**:254.

738 Emerson D, Moyer C. Isolation and characterization of novel iron-oxidizing bacteria

739   that grow at circumneutral pH. *Appl Environ Microbiol* 1997;**63**:4784–92.

740 Emerson D, Scott JJ, Benes J *et al.* Microbial iron oxidation in the Arctic tundra and

741   its implications for biogeochemical cycling. *Appl Environ Microbiol*

742   2015;**81**:8066–75.

743 Evans KA, Watkins DC, Banwart SA. Rate controls on the chemical weathering of

744   natural polymineralic material. II. Rate-controlling mechanisms and mineral

745   sources and sinks for element release from four UK mine sites, and implications

746   for comparison of laboratory and field scale weathering. *Appl Geochemistry*

747   2006;**21**:377–403.

748 Fabisch M, Beulig F, Akob DM *et al.* Surprising abundance of Gallionella-related

749   iron oxidizers in creek sediments at pH 4.4 or at high heavy metal

750   concentrations. *Front Microbiol* 2013;**4**:390.

751 Fabisch M, Freyer G, Johnson CA *et al.* Dominance of "Gallionella

752   capsiferriformans" and heavy metal association with Gallionella-like stalks in

753   metal-rich pH 6 mine water discharge. *Geobiology* 2016;**14**:68–90.

754 Farr G, Sadasivam S, Manju *et al.* Low enthalpy heat recovery potential from coal

755   mine discharges in the South Wales Coalfield. *Int J Coal Geol* 2016;**164**:92–103.

756 Faure G. *Principles and Applications of Geochemistry*. New Jersey: Prentice Hall,

757   1998.

758 Finneran KT, Johnsen C V, Lovley DR. Rhodoferax ferrireducens sp. nov., a

759   psychrotolerant, facultatively anaerobic bacterium that oxidizes acetate with the

760   reduction of Fe(III). *Int J Syst Evol Microbiol* 2003;**53**:669–73.

761 Fleming EJ, Cetinić I, Chan CS *et al.* Ecological succession among iron-oxidizing

762   bacteria. *ISME J* 2014;**8**, DOI: 10.1038/ismej.2013.197.

763 Fleming EJ, Langdon AE, Martinez-Garcia M *et al.* What's New Is Old: Resolving

764   the Identity of Leptothrix ochracea Using Single Cell Genomics, Pyrosequencing

765 and FISH. Stal L (ed.). *PLoS One* 2011;**6**:e17769.

766 Gadd GM. Microbial influence on metal mobility and application for bioremediation.

767 *Geoderma* 2004;**122**:109–19.

768 Good IJ. The population frequencies of species and the estimation of population

769 parameters. *Biometrika* 1953;**40**:237–64.

770 Haas BJ, Gevers D, Earl AM *et al.* Chimeric 16S rRNA sequence formation and

771 detection in Sanger and 454-pyrosequenced PCR amplicons. *Genome Res*

772 2011;**21**:494–504.

773 Hallbeck L, Pedersen K. Autotrophic and mixotrophic growth of Gallionella

774 ferruginea. *J Gen Microbiol* 1991;**137**:2657–61.

775 Hallberg KB, Johnson DB. Novel acidophiles isolated from moderately acidic mine

776 drainage waters. *Hydrometallurgy* 2003;**71**:139–48.

777 Hedrich S, Schlömann M, Barrie Johnson D. The iron-oxidizing proteobacteria.

778 *Microbiology* 2011, DOI: 10.1099/mic.0.045344-0.

779 von der Heyden BP, Hauser EJ, Mishra B *et al.* Ubiquitous Presence of Fe(II) in

780 Aquatic Colloids and Its Association with Organic Carbon. *Environ Sci Technol*

781 *Lett* 2014;**1**:387–92.

782 Hohmann C, Winkler E, Morin G *et al.* Anaerobic Fe(II)-Oxidizing Bacteria Show As

783 Resistance and Immobilize As during Fe(III) Mineral Precipitation. *Environ Sci*

784 *Technol* 2010;**44**:94–101.

785 Hopwood MJ, Statham PJ, Skrabal SA *et al.* Dissolved iron(II) ligands in river and

786 estuarine water. *Mar Chem* 2015;**173**:173–82.

787 Ionescu D, Heim C, Polerecky L *et al.* Biotic and abiotic oxidation and reduction of

788 iron at circumneutral pH are inseparable processes under natural conditions.

789 *Geomicrobiol J* 2015;**32**:221–30.

790   Islam FS, Gault AG, Boothman C *et al.* Role of metal-reducing bacteria in arsenic

791   release from Bengal delta sediments. *Nature* 2004;**430**:68–71.

792   Johnson DB, Hallberg KB. The microbiology of acidic mine waters. *Res Microbiol*

793   2003;**154**:466–73.

794   Kappler A, Schink B, Newman DK. Fe(III) mineral formation and cell encrustation

795   by the nitrate-dependent Fe(II)-oxidizer strain BoFeN1. *Geobiology* 2005;**3**:235–

796   45.

797   Keim CN. Arsenic in Biogenic Iron Minerals from a Contaminated Environment.

798   *Geomicrobiol J* 2011;**28**:242–51.

799   Kleja DB, van Schaik JWJ, Persson I *et al.* Characterization of iron in floating surface

800   films of some natural waters using EXAFS. *Chem Geol* 2012;**326**–**327**:19–26.

801   Klindworth A, Pruesse E, Schweer T *et al.* Evaluation of general 16S ribosomal RNA

802   gene PCR primers for classical and next-generation sequencing-based diversity

803   studies. *Nucleic Acids Res* 2013;**41**:e1.

804   Kuczynski J, Stombaugh J, Walters WA *et al.* Using QIIME to Analyze 16S rRNA

805   Gene Sequences from Microbial Communities. *Current Protocols in*

806   *Bioinformatics*. Vol Chapter 10. Hoboken, NJ, USA: John Wiley & Sons, Inc.,

807   2011, Unit 10.7.

808   Lane DJ. 16S/23S rRNA Sequencing. *Nucleic Acid Techniques in Bacterial*

809   *Systematic*. 1991.

810   Laufer K, Byrne JM, Glombitza C *et al.* Anaerobic microbial Fe(II) oxidation and

811   Fe(III) reduction in coastal marine sediments controlled by organic carbon

812   content. *Environ Microbiol* 2016a;**18**:3159–74.

813   Laufer K, Nordhoff M, Røy H *et al.* Coexistence of microaerophilic, nitrate-reducing,

814   and phototrophic Fe(II) oxidizers and Fe(III) reducers in coastal marine

815   sediment. *Appl Environ Microbiol* 2016b;**82**:1433–47.

816   Laufer K, Røy H, Jørgensen BB *et al.* Evidence for the Existence of Autotrophic

817   Nitrate-Reducing Fe(II)-Oxidizing Bacteria in Marine Coastal Sediment. Kostka

818   JE (ed.). *Appl Environ Microbiol* 2016c;**82**:6120–31.

819   Lewis BJ, Leighfield KG, Cox SJ. *The South Wales Coalfield (Including the*

820   *Pembrokeshire Coalfield): A Review of Mine Water Recovery. Report from*

821   *Wardell Armstrong for Coal Authority, Job NL02906.*, 2000.

822   Lloyd JR. Microbial reduction of metals and radionuclides. *FEMS Microbiol Rev*

823   2003;**27**:411–25.

824   Lovley DR. Microbial Fe(III) reduction in subsurface environments. *FEMS Microbiol*

825   *Rev* 1997;**20**:305–13.

826   Lovley DR, Phillips EJP. Novel Mode of Microbial Energy Metabolism: Organic

827   Carbon Oxidation Coupled to Dissimilatory Reduction of Iron or Manganese.

828   *Appl Environ Microbiol* 1988;**54**:1472–80.

829   Lueder U, Druschel G, Emerson D *et al.* Quantitative analysis of O2 and Fe2+

830   profiles in gradient tubes for cultivation of microaerophilic Iron(II)-oxidizing

831   bacteria. *FEMS Microbiol Ecol* 2018;**94**, DOI: 10.1093/femsec/fix177.

832   Melton ED, Swanner ED, Behrens S *et al.* The interplay of microbially mediated and

833   abiotic reactions in the biogeochemical Fe cycle. *Nat Rev Microbiol*

834   2014;**12**:797–808.

835   Mesa V, Gallego JLR, González-Gil R *et al.* Bacterial, Archaeal, and Eukaryotic

836   Diversity across Distinct Microhabitats in an Acid Mine Drainage. *Front*

837   *Microbiol* 2017;**8**:1756.

838   Muehe EM, Kappler A. Arsenic mobility and toxicity in South and South-east Asia –

839   a review on biogeochemistry, health and socio-economic effects, remediation

840   and risk predictions. *Environ Chem* 2014;**11**:483.

841   Neubauer SC, Emerson D, Megonigal JP. Life at the energetic edge: kinetics of

842   circumneutral iron oxidation by lithotrophic iron-oxidizing bacteria isolated from

843   the wetland-plant rhizosphere. *Appl Environ Microbiol* 2002;**68**:3988–95.

844   Nevin KP, Holmes DE, Woodard TL *et al.* Geobacter bemidjiensis sp. nov. and

845   Geobacter psychrophilus sp. nov., two novel Fe(III)-reducing subsurface

846   isolates. *Int J Syst Evol Microbiol* 2005;**55**:1667–74.

847   Nordstrom DK, Alpers CN. Negative pH, efflorescent mineralogy, and consequences

848   for environmental restoration at the Iron Mountain Superfund site, California.

849   *Proc Natl Acad Sci U S A* 1999;**96**:3455–62.

850   Otte JM, Harter J, Laufer K *et al.* The distribution of active iron-cycling bacteria in

851   marine and freshwater sediments is decoupled from geochemical gradients.

852   *Environ Microbiol* 2018;**20**:2483–99.

853   Overmann J. The Family Chlorobiaceae. *The Prokaryotes*. New York, NY: Springer

854   New York, 2006, 359–78.

855   Park B, Dempsey BA. Heterogeneous oxidation of Fe(II) on ferric oxide at neutral pH

856   and a low partial pressure of O2. *Environ Sci Technol* 2005;**39**:6494–500.

857   Parkhurst DL, Appelo CAJ. *User's Guide To PHREEQC (Version 2) — a Computer

858   Program for Speciation, and Inverse Geochemical Calculations.*, 1999.

859   Peine A, Tritschler A, Küsel K *et al.* Electron flow in an iron-rich acidic sediment-

860   evidence for an acidity-driven iron cycle. *Limnol Oceanogr* 2000;**45**:1077–87.

861   Percent SF, Frischer ME, Vescio PA *et al.* Bacterial Community Structure of Acid-

862   Impacted Lakes: What Controls Diversity? *Appl Environ Microbiol*

863   2008;**74**:1856–68.

864   Pereira LB, Vicentini R, Ottoboni LMM. Changes in the Bacterial Community of Soil

from a Neutral Mine Drainage Channel. Moustafa A (ed.). *PLoS One* 2014;**9**:e96605.

Quatrini R, Johnson DB. Microbiomes in extremely acidic environments: functionalities and interactions that allow survival and growth of prokaryotes at low pH. *Curr Opin Microbiol* 2018;**43**:139–47.

Reiche M, Lu S, Ciobotă V *et al.* Pelagic boundary conditions affect the biological formation of iron-rich particles (iron snow) and their microbial communities. *Limnol Oceanogr* 2011;**56**:1386–98.

Rhine ED, Garcia-Dominguez E, Phelps CD *et al.* Environmental microbes can speciate and cycle arsenic. *Environ Sci Technol* 2005;**39**:9569–73.

Robins NS, Davies J, Dumpleton S. Groundwater flow in the South Wales coalfield: historical data informing 3D modelling. *Q J Eng Geol Hydrogeol* 2008;**41**:477–86.

Roden EE. Microbial iron-redox cycling in subsurface environments. *Biochem Soc Trans* 2012;**40**:1249–56.

Roden EE, McBeth JM, Blöthe M *et al.* The Microbial Ferrous Wheel in a Neutral pH Groundwater Seep. *Front Microbiol* 2012;**3**:172.

Sapsford D, Santonastaso M, Thorn P *et al.* Conversion of coal mine drainage ochre to water treatment reagent: Production, characterisation and application for P and Zn removal. *J Environ Manage* 2015;**160**:7–15.

Satola B, Wübbeler JH, Steinbüchel A. Metabolic characteristics of the species Variovorax paradoxus. *Appl Microbiol Biotechnol* 2013;**97**:541–60.

Schink B. Synergistic interactions in the microbial world. *Antonie Van Leeuwenhoek* 2002;**81**:257–61.

Schmidt C, Behrens S, Kappler A. Ecosystem functioning from a geomicrobiological

890   perspective – a conceptual framework for biogeochemical iron cycling. *Environ*

891   *Chem* 2010;**7**:399.

892   Shannon CE. The mathematical theory of communication. *Bell Syst Tech J*

893   1948;**27**:623–56.

894   Smedley P., Kinniburgh D. A review of the source, behaviour and distribution of

895   arsenic in natural waters. *Appl Geochemistry* 2002;**17**:517–68.

896   Smedley PL, Kinniburgh DG. Arsenic in groundwater and the environment.

897   *Essentials of Medical Geology: Revised Edition*. 2013.

898   Sowers TD, Harrington JM, Polizzotto ML *et al.* Sorption of arsenic to biogenic iron

899   (oxyhydr)oxides produced in circumneutral environments. *Geochim Cosmochim*

900   *Acta* 2017;**198**:194–207.

901   Stams AJM, Plugge CM. Electron transfer in syntrophic communities of anaerobic

902   bacteria and archaea. *Nat Rev Microbiol* 2009;**7**:568–77.

903   Stookey LL. Ferrozine-A New Spectrophotometric Reagent for Iron. *Anal Chem*

904   1970;**42**:779–81.

905   Stumm W, Morgan JJ. *Aquatic Chemistry: Chemical Equilibria and Rates in Natural*

906   *Waters.*, 1993.

907   Sundman A, Karlsson T, Laudon H *et al.* XAS study of iron speciation in soils and

908   waters from a boreal catchment. *Chem Geol* 2014;**364**:93–102.

909   Vaughan DJ, Lloyd JR. Mineral-organic-microbe interactions: Environmental impacts

910   from molecular to macroscopic scales. *Comptes Rendus Geosci* 2011;**343**:140–

911   59.

912   Volant A, Bruneel O, Desoeuvre A *et al.* Diversity and spatiotemporal dynamics of

913   bacterial communities: physicochemical and other drivers along an acid mine

914   drainage. *FEMS Microbiol Ecol* 2014;**90**:247–63.

915   Wang X-J, Yang J, Chen X-P *et al.* Phylogenetic diversity of dissimilatory ferric iron

916   reducers in paddy soil of Hunan, South China. *J Soils Sediments* 2009;**9**:568–77.

917   Waters CN, Waters RA, Barclay WJ *et al. A Lithostratigraphical Framework for the*

918   *Carboniferous Successions of Southern Great Britain (Onshore). British*

919   *Geological Survey Research Report, RR/09/01.*, 2009.

920   Whiteley AS, Jenkins S, Waite I *et al.* Microbial 16S rRNA Ion Tag and community

921   metagenome sequencing using the Ion Torrent (PGM) Platform. *J Microbiol*

922   *Methods* 2012;**91**:80–8.

923   Widdel F, Schnell S, Heising S *et al.* Ferrous iron oxidation by anoxygenic

924   phototrophic bacteria. *Nature* 1993;**362**:834–6.

925   Willems A, De Ley J, Gillis M *et al.* Comamonadaceae, a New Family Encompassing

926   the Acidovorans rRNA Complex, Including Variovorax paradoxus gen. nov.,

927   comb. nov., for Alcaligenes paradoxus (Davis 1969). *Int J Syst Bacteriol*

928   1991;**41**:445–50.

929   Wilson AD. A new method for the determination of ferrous iron in rocks and

930   minerals. *Bull Geol Surv Gt Britain* 1955;**9**:55–8.

931   Wittebolle L, Marzorati M, Clement L *et al.* Initial community evenness favours

932   functionality under selective stress. *Nature* 2009;**458**:623–6.

933   Wragg J. Certificate of Analysis: BGS Guidance Material 102 Ironstone Soil. 2009.

934   Yao W, Millero FJ. Oxidation of hydrogen sulfide by hydrous Fe(III) oxides in

935   seawater. *Mar Chem* 1996;**52**:1–16.

936   Younger PL. The longevity of minewater pollution: A basis for decision-making. *Sci*

937   *Total Environ* 1997;**194**–**195**:457–66.

938

939

940   Figures and Tables

Geological information, BGS © NERC.
Contains Ordnance Survey data © Crown Copyright and database rights 2018
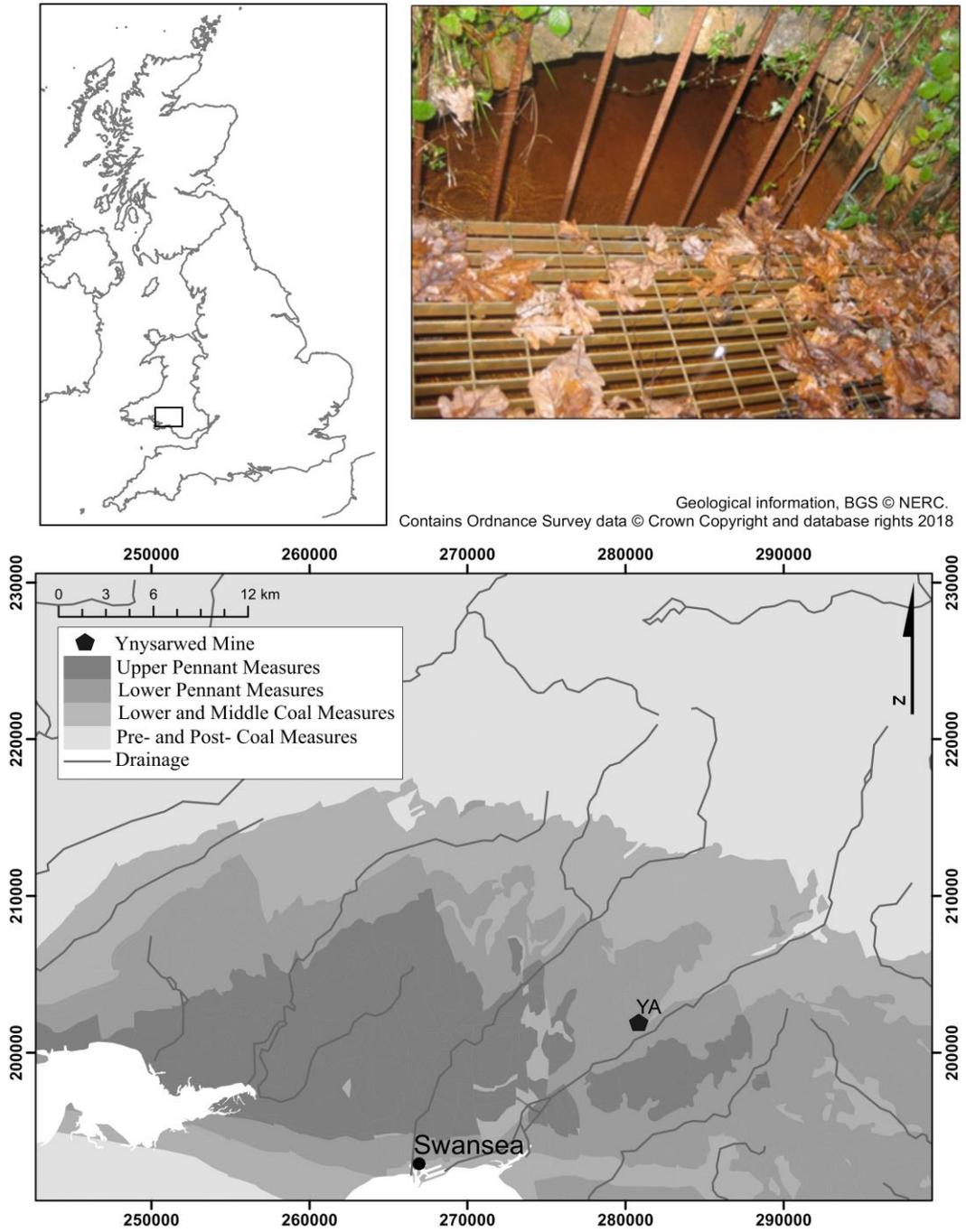
941

942   Figure 1: Sampling location at the Ynysarwed mine adit in the South Wales Coalfield,

943   UK.

944
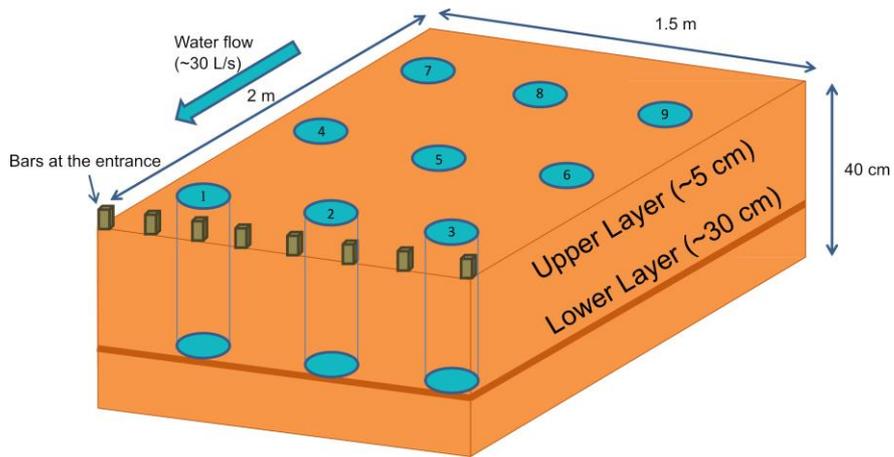
945

946

947 Figure 2: Schematic of high resolution sampling strategy within the Fe-rich deposit at

948 the Ynysarwed mine adit in the South Wales Coalfield, UK.

949
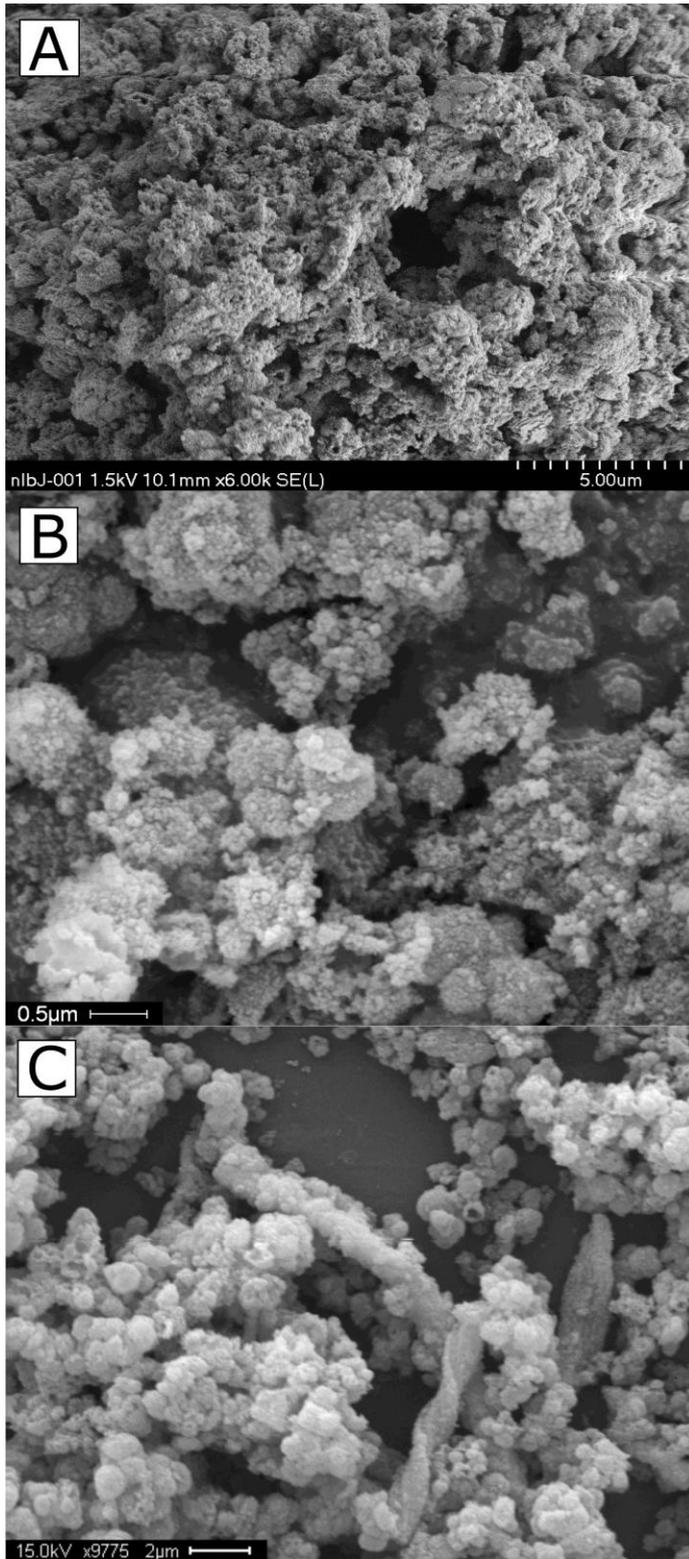
950

951   Figure 3: Electron microscopy micrographs of natural precipitates at the Ynysarwed

952   mine adit showing poorly-crystalline Fe minerals by (A) SEM, (B) ESEM (high

953   vacuum), and (C) ESEM (high vacuum) showing Fe minerals and twisted

954   *Gallionella*-like stalks.
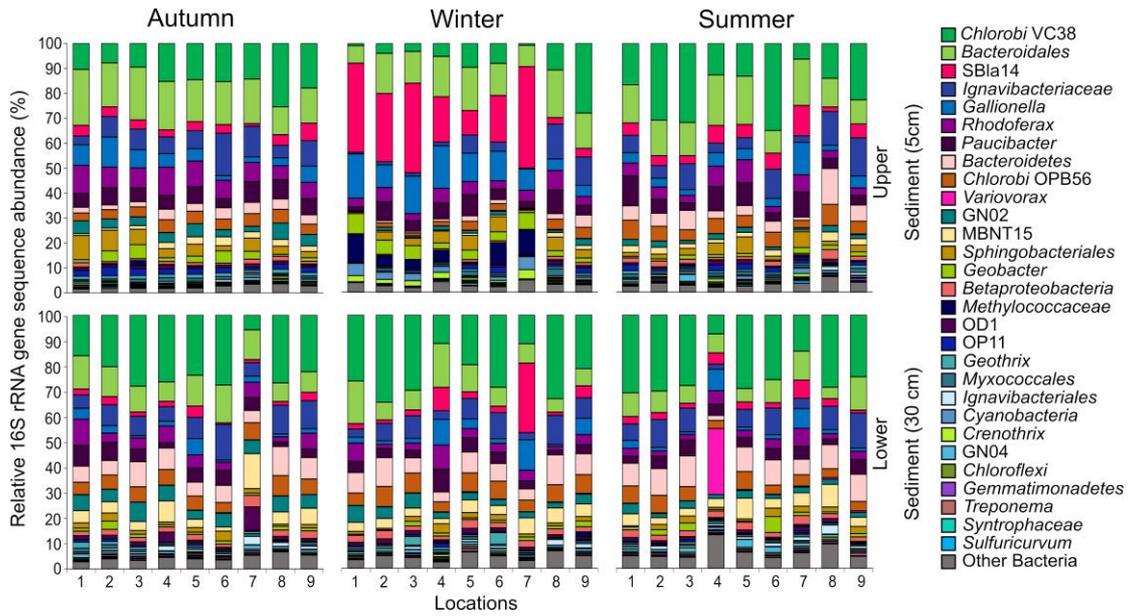
Figure 4: Relative 16S rRNA gene sequence abundance of bacterial groups in samples collected from the Ynysarwed mine at locations 1 to 9 in the upper (5 cm depth) and lower (30 cm depth) sediments in autumn (October 2011), winter (February 2012) and summer (July 2012). Bacterial groups were produced by clustering OTUs together based on their lowest level classification following QIIME analysis.

963
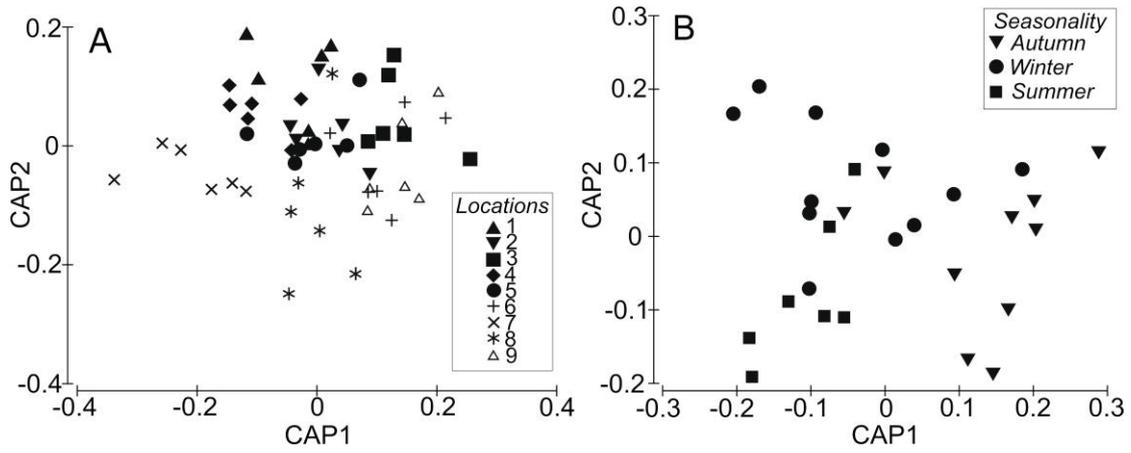
Figure 5: Bacterial community diversity according to A) locations and B) seasons

based on Bray-Curtis distances of fourth root transformed abundance data.

966

967
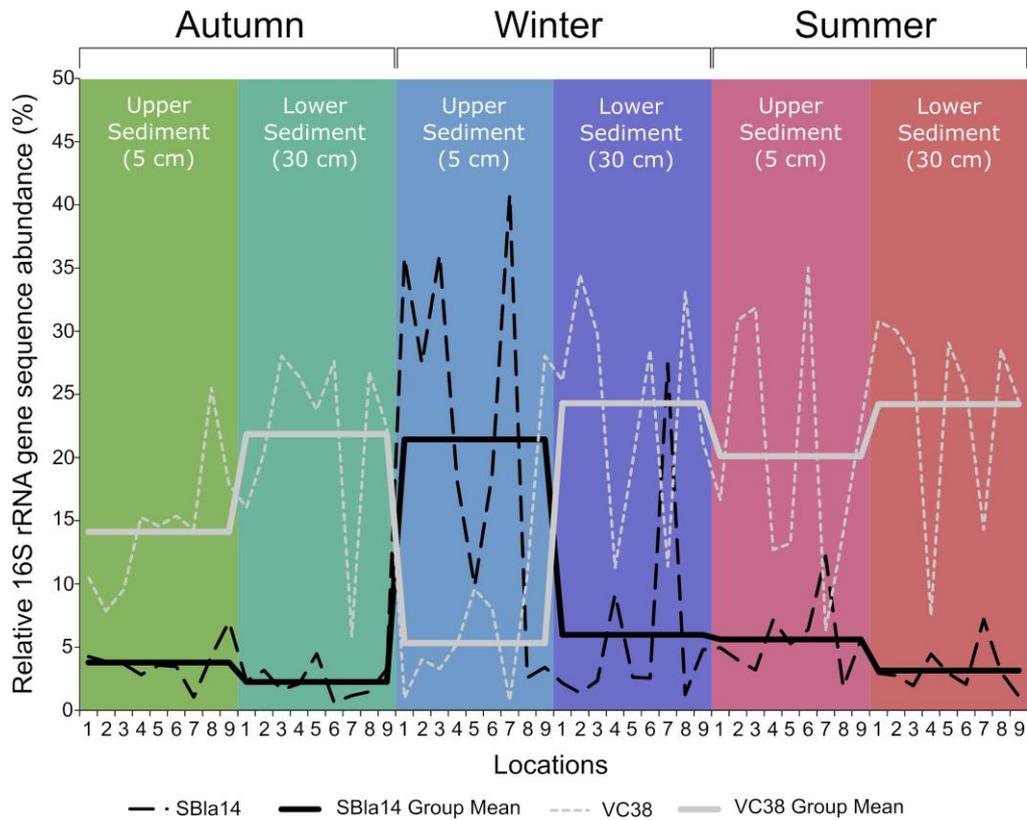
Figure 6: A bloom of the *Betaproteobacterial* order SB1a14 and a concomitant decrease in *Chlorobi* order VC38 in the upper (5 cm) sediment layer during winter (February 2012). Samples were grouped according to month and depth and a mean abundance ($n = 9$) for both taxa was calculated. Numbers refer to the location of the sample.

975 Table 1: General overview of geochemical parameters at the Ynysarwed mine site for

976 the mine water, sediment, and sediment porewater. Samples were collected in autumn

977 (October 2011), winter (February 2012), and summer (July 2012). Sediment and

978 porewater data show mean values for 18 samples collected each timepoint. Bdl is

979 below detection limit.

980

Parameter	Sample Type	Mean (min - max)		
		Autumn	Winter	Summer
pH	Mine Water	6.2	6.1	6.3
Temperature (°C)		13.8	12.3	15.6
Eh (mV)		8.6	14.2	37.5
Conductivity ($\mu S\ cm^{-1}$)		1212	1131	1173
Fe^{total} (mg L^{-1})		64.5 ± 1.9	55.3 ± 1.7	47.1 ± 1.4
Ca (mg L^{-1})		148 ± 1.9	140 ± 1.8	154 ± 2.0
Mg (mg L^{-1})		73.7 ± 2.5	72.4 ± 2.5	70 ± 2.4
Na (mg L^{-1})		74.5 ± 2.6	72 ± 2.5	77.5 ± 2.7
K (mg L^{-1})		19.8 ± 0.6	16.4 ± 0.5	21.2 ± 0.6
As^{total} (ug L^{-1})		19.5 ± 0.3	27.3 ± 0.4	29.7 ± 0.4
SO_4^{2-} (mg L^{-1})		352 ± 7.7	931 ± 20.5	844 ± 18.6
NO_3^- (mg L^{-1})		bdl	bdl	bdl
HCO_3^- (mg L^{-1})		248 ± 6.1	40 ± 0.1	109 ± 2.27
pH	Sediment	5.3 (5.2 - 5.4)	6.3 (6.2 - 6.4)	6.3 (6.1 - 6.4)
Fe (%) in sediment		42.5 (38.4 - 48.1)	57.4 (48.7 - 63.7)	56.6 (52.7 - 61.1)
As in sediment (mg kg^{-1})		1868 (1410 - 2252)	1228 (937 - 1356)	1230 (872 - 1439)
Ca in sediment (mg kg^{-1})		512 (211 - 2110)	2722 (1433 - 5092)	2195 (1361 - 3337)
Organic matter (%)		16.2 (12.5 - 34.3)	11.1 (9.9 - 12.5)	6.5 (5.8 - 9.9)
Fe(II) in porewater (mg L^{-1})	Pore Water	33.3 (19.9 - 47.1)	39.3 (13.2 - 49.5)	22.9 (<1 - 60.1)

981

982

983

984   Table 2: Summary results for alpha diversity metrics for all 54 samples collected from

985   the Ynysarwed mine adit calculated using the QIIME software package. (Note:

986   Shannon values were converted from the QIIME output as the software calculates the

987   metric to log base 2 not the natural log. Therefore, all output values were multiplied

988   by 0.69315).

989

Alpha Diversity Metric	Mean	Minimum	Maximum	Median
Chao1	93.3	80.2	98.3	94
Good's Coverage	100	100	100	100
Observed Species	92.3	79	95	93
Gini Index	0.7	0.6	0.8	0.7
Shannon	3.3	2.8	3.7	3.3

990

991

992

993   Figure S1: XRD pattern for Fe-rich sediment collected at the Ynysarwed mine adit

994   with the sample (black line) and the standard reference for goethite (red line). The

995   broad reflection between 5° and 30° is due to the kapton film used to prevent drying

996   of sample during analysis.
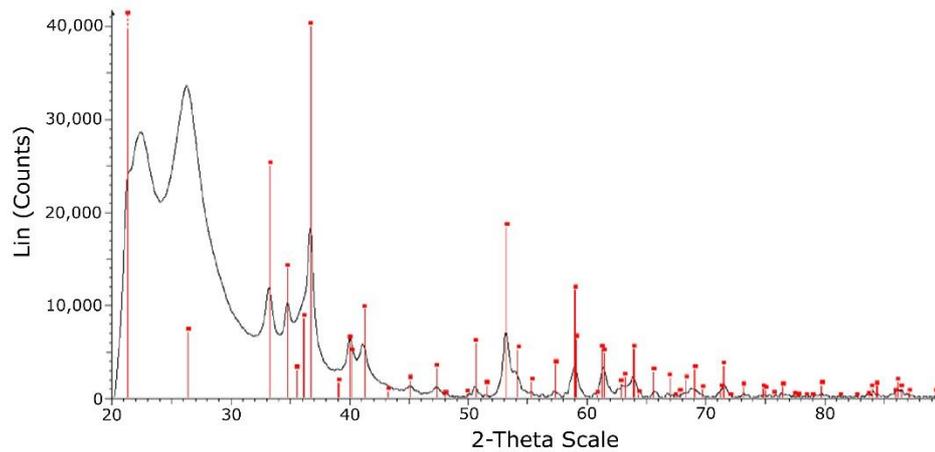
997

998

999

1000 Figure S2: Bacterial communities at phylum level within the Ynysarwed mine adit

1001 according to depth. The mean values are taken for 27 samples each in the upper and

1002 lower sediments.

1003
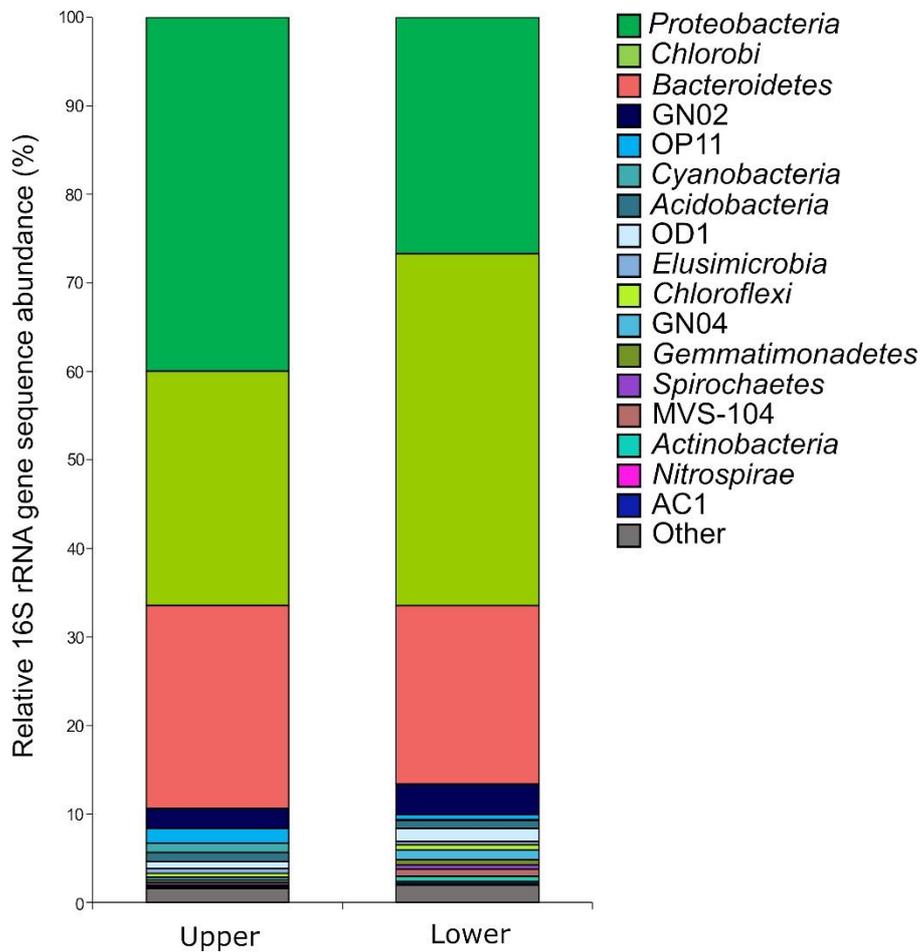
1004

1005

1006

1007   Figure S3: Bacterial communities at phylum level within the Ynysarwed sediment

1008   according to month using mean values of 18 samples per month in autumn (October

1009   2011), winter (February 2012), and summer (July 2012).

1010
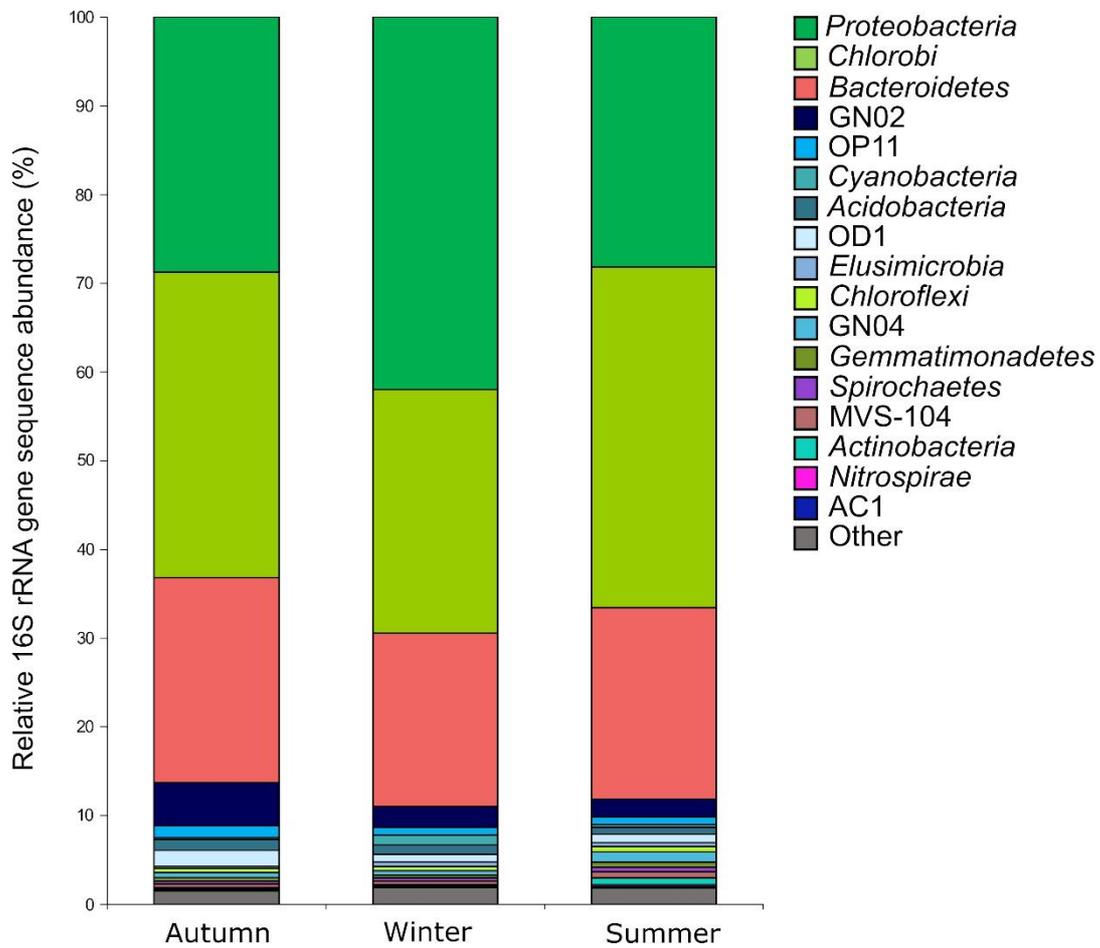
1011

1012

1013

1014   Figure S4: Non-metric multidimensional scaling (nMDS) of bacterial community

1015   diversity according to seasons based on Bray-Curtis distances of fourth root

1016   transformed abundance data.
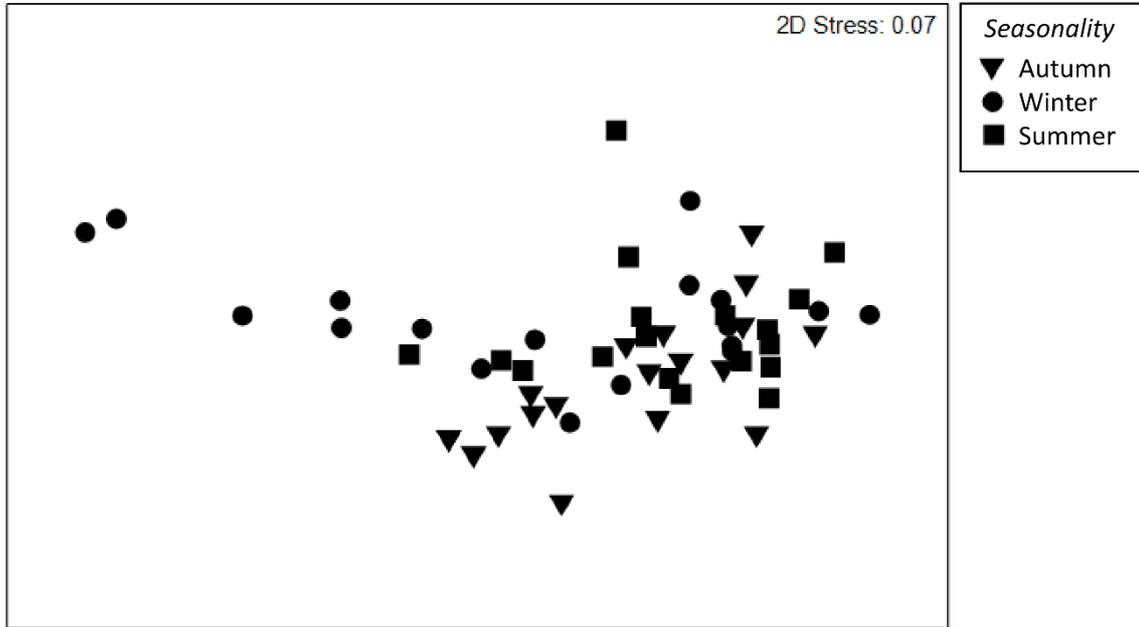
1017

1018

1019   Table S1: Geochemical analysis of samples collected from the Ynysarwed mine site

1020   sediment in autumn (October 2011), winter (February 2012), and summer (July

1021   2012). A is autumn, W is winter; S is summer; OM is organic matter; numbers 1-9

1022   refer to sample location within the Fe(III) deposit; U is upper sediments (5 cm depth);

1023   L is lower sediments (30 cm depth); nd is no data available

1024

Sample	Fe^{total} weight %			Weight % Fe^{2+} of Fe^{total}			pH			OM weight %			Porewater Fe(II) (mg L^{-1})		
	A	W	S	A	W	S	A	W	S	A	W	S	A	W	S
1U	42.1	56.6	56.0	nd	0.0	1.2	nd	6.4	6.3	16.0	10.5	6.7	29	49	0
2U	44.1	55.0	61.1	nd	1.2	1.0	5.4	nd	6.2	15.4	10.2	8.0	27	33	2
3U	45.4	53.4	60.9	nd	2.7	1.3	nd	nd	nd	15.1	11.7	8.0	33	13	2
4U	46.7	57.8	56.5	nd	1.2	0.4	nd	nd	6.4	34.3	12.2	6.5	33	40	2
5U	41.9	57.3	52.7	nd	1.1	1.1	nd	6.4	6.4	nd	10.0	5.9	*43*	32	1
6U	44.4	57.2	55.1	nd	1.3	1.0	nd	nd	6.4	16.4	12.2	6.1	30	39	1
7U	38.7	59.6	57.0	nd	0.3	0.3	5.5	6.5	6.4	13.6	10.1	8.5	31	31	56
8U	38.6	60.4	58.0	nd	0.0	0.6	nd	6.4	6.5	nd	12.4	9.3	*35*	44	43
9U	44.2	58.5	55.6	nd	0.0	0.6	nd	6.4	nd	nd	12.1	6.7	*20*	32	31
1L	41.8	48.7	56.0	nd	0.1	0.4	5.4	6.3	6.3	12.6	10.0	7.5	37	43	2
2L	48.1	59.7	58.0	nd	0.4	0.6	5.4	6.2	6.2	13.6	10.2	8.1	37	49	51
3L	41.7	60.2	54.3	nd	0.2	0.4	nd	6.4	6.3	nd	10.1	7.0	*35*	45	8
4L	41.0	63.8	57.2	nd	0.0	1.1	nd	6.3	6.3	nd	12.1	10.0	*47*	43	51
5L	41.1	60.7	54.9	nd	0.5	1.5	nd	6.3	6.3	nd	11.3	7.3	*40*	46	57
6L	43.2	60.2	55.1	nd	0.4	1.8	nd	6.3	6.3	nd	10.9	7.6	*32*	45	41
7L	38.3	58.8	56.1	nd	0.2	1.5	5.4	6.3	6.3	12.5	10.4	9.6	28	31	1
8L	43.4	58.8	55.7	nd	0.7	1.5	5.4	6.3	6.3	15.0	10.7	9.9	31	47	60
9L	41.6	49.6	59.9	nd	0.7	1.6	5.2	6.2	6.1	14.3	12.5	8.7	32	44	4

1025
1026

1027

1028

1029

1030   Table S2: Pairwise PERMANOVA comparisons of selected phyla diversity for the

1031   main effects of month and depth calculated based on the summed relative abundance

1032   of selected phyla. Significant differences are shown in bold whilst highly significant

1033   differences are underlined.

Phylum	Pairwise Tests							
	Pairwise *t* statistic				Pairwise *P* value			
	Upper x Lower	Oct x Feb	Oct x Jul	Feb x Jul	Upper x Lower	Oct x Feb	Oct x Jul	Feb x Jul
Proteobacteria	4.6252	2.8597	0.5494	2.7688	**<u>0.0008</u>**	**0.0225**	0.6026	**0.0233**
Chlorobi	4.6932	3.0977	0.7772	3.6309	**<u>0.0002</u>**	**0.0124**	0.453	**<u>0.0049</u>**
Bacteroidetes	1.7471	2.0306	1.2331	1.1475	0.0985	0.0795	0.2504	0.2875

1034

1035

1036

1037   Dataset S1: Heatmap showing the relative 16S rRNA gene sequence abundance of

1038   bacterial communities at OTU level in samples collected from the Ynysarwed mine at

1039   locations 1 to 9 in the upper and lower sediments in autumn (October 2011), winter

1040   (February 2012), and summer (July 2012).

1041